Astrophysical reaction rate for the $^{18}F(p,\alpha)^{15}O$ reaction

K. E. Rehm,[1] M. Paul,[2] A. D. Roberts,[3] C. L. Jiang,[1] D. J. Blumenthal,[1] S. M. Fischer,[1] J. Gehring,[1] D. Henderson,[1] J. Nickles,[3] J. Nolen,[1] R. C. Pardo,[1] J. P. Schiffer,[1] and R. E. Segel[4]

[1]*Argonne National Laboratory, Argonne, Illinois 60439*

[2]*Hebrew University, Jerusalem, Israel*

[3]*University of Wisconsin, Madison, Wisconsin 53706*

[4]*Northwestern University, Evanston, Illinois 60208*

(Received 13 November 1995)

An excitation function for the $^{18}F(p,\alpha)^{15}O$ reaction has been measured in the energy range $E_{c.m.}=600-800$ keV using a radioactive ^{18}F beam. A resonant state with a spin value of $3/2^+$ has been found at an energy of 652 keV above threshold. This $l_p=0$ resonance is found to dominate the astrophysical reaction rate at temperatures $T_9>0.5$.

PACS number(s): 25.60.Je, 25.70.Ef, 26.30.+k, 27.20.+n

I. INTRODUCTION

Experiments with radioactive ion beams have opened new opportunities for the study of reaction processes which are important for our understanding of explosive nucleosynthesis [1]. Explosive nucleosynthesis is thought to occur in the Universe at various sites including nova and supernova explosions. The recent detection of γ lines from the decay of ^{26}Al in the interstellar medium [2] and of ^{56}Ni in SN 1987a [3] provides experimental evidence for the nuclear processes taking place in the universe. The synthesis of heavier elements in explosive nucleosynthesis in a proton-rich environment is believed to proceed through the nuclide ^{19}Ne which is produced either directly via the $^{15}O(\alpha,\gamma)^{19}Ne$ reaction or via the $^{14}O(\alpha,p)^{17}F$ reaction followed by the sequence $^{17}F(p,\gamma)^{18}Ne(\beta^+)^{18}F(p,\gamma)^{19}Ne$. ^{19}Ne is then the starting point for the rp process producing nuclei up to ^{56}Ni and beyond [4]. In the reaction chain starting with proton capture by ^{17}F, however, there is a competing reaction, $^{18}F(p,\alpha)^{15}O$, which recycles material back into the CNO cycle. How ^{18}F interacts with protons at low energies is therefore of key interest for controlling the breakout from the ''hot CNO cycle'' into the rp process. This is evidenced by recent network calculations [1,5] which show a strong dependence of the reaction flow on the $^{18}F(p,\alpha)^{15}O$ rate. For this reason a measurement of the $^{18}F(p,\alpha)$ cross section is needed requiring the development of radioactive ^{18}F beams.

During the last year two studies of the $^{18}F(p,\alpha)^{15}O$ reaction have been reported. In one experiment, using a tandem accelerator, the heavy reaction partner (^{15}O) was detected with a magnetic spectrograph [6,7], while in the other, using a cyclotron, the α particle was measured in an annular array of Si detectors [8,9]. Both experiments identified a $3/2^+$ state at an energy about 650 keV above threshold. The location of this $3/2^+$ state differed slightly in the two publications. While in [7] an energy of 655 keV above the threshold was assumed based on measurements of the $^{19}F(^3He,t)^{19}Ne$ reaction [10], the results of [8] gave an energy of 638 ± 15 keV. In a new set of experiments using the same technique as in [7] and utilizing the easy energy variability of a tandem accelerator we have measured an excitation function for the $^{18}F(p,\alpha)^{15}O$ reaction. The results obtained for the resonance strength and the excitation energy are then used to calculate the astrophysical reaction rate.

II. EXPERIMENTAL DETAILS

The experiments were performed using a two-stage method for producing the ^{18}F beam. Aqueous $^{18}F^-$ ions are produced at the University of Wisconsin cyclotron via the $^{18}O(p,n)^{18}F$ reaction with 11 MeV protons bombarding an enriched [^{18}O] water target. After replacing the [^{18}O] water with [^{16}O] water by azeotropic distillation, the ^{18}F is deposited on the surface of an Al/Ag plug which is pressed into the copper cathode insert for a negative-ion Cs-sputter source (SNICS National Electrostatics Corporation). The cathode is then flown to Argonne and installed in the ion source of the tandem accelerator of ATLAS. A more detailed description of the production method can be found in [11]. The number of ^{18}F atoms in the ion source was between 5 and 10×10^{13}, corresponding to an initial activity of 150–300 mCi. The overall efficiency for extracting ^{18}F ions from the source material to the tandem injection line ranged in the recent experiments from 0.1 to 1 %. This represents an improvement by a factor of $\sim$10 over previous experiments and is due to a reduction of the Cs-sputter rate in the SNICS source by operating the source at lower ionizer currents. The use of solid ^{18}F material in the ion source seems to be advantageous since test measurements with gaseous CH_3F resulted in a source efficiency of only 3×10^{-4}.

The ^{18}F ions in their 4^+ state were accelerated with the tandem accelerator to energies between 11.7 and 15.1 MeV. The transmission efficiency of the FN tandem accelerator operating at terminal voltages below 3 MV as determined from a comparison of the currents at the ion source and at the target, respectively, is strongly energy dependent and is generally only 1–10 %, so that only $2-6\times10^9$ ^{18}F are transmitted to the target. For a typical run of 2 h this corresponds to an average beam current on target of $\sim5\times10^5$ ^{18}F/sec. Since the beam transport system does not separate $^{18}F^{4+}$ ions from the stable isobar $^{18}O^{4+}$ the ^{18}F beam has a considerable admixture of ^{18}O with an intensity which is $\sim$500–2000 times stronger.

Thin stretched polypropylene foils ($\sim$60 $\mu g/cm^2$) were

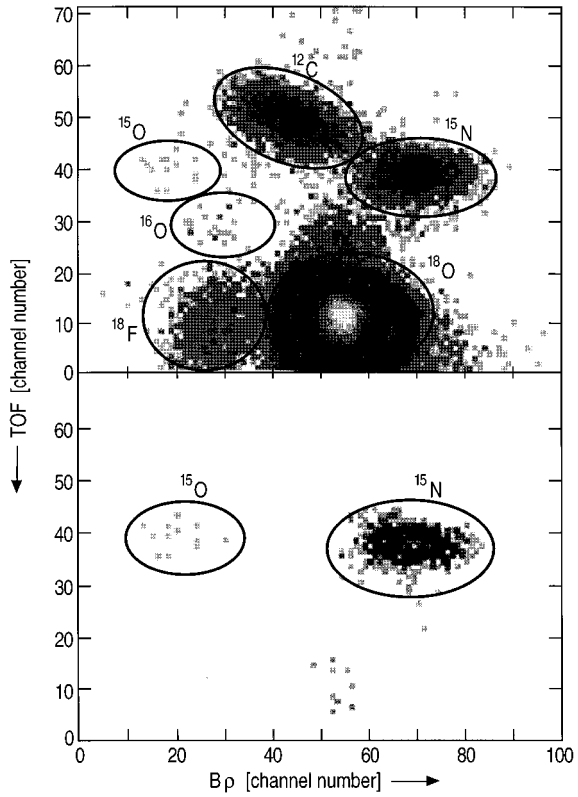

FIG. 1. (a) Two-dimensional plot of time of flight (TOF) vs magnetic rigidity ($B\rho$) measured with the gas-filled magnet and the Si-strip detector array in the focal plane. The energy of the ^{18}O-^{18}F beam was 12.4 MeV. The various particle groups are indicated. (b) Same as (a) but with the additional requirement of a coincident particle in the recoil detector located at $\theta_{lab}=60°$. Because the recoil angle was chosen for the $p(^{18}F, ^{15}O)\alpha$ reaction only a fraction of the ^{15}N originating from the $p(^{18}O, ^{15}N)\alpha$ reaction are detected in the coincidence spectrum.

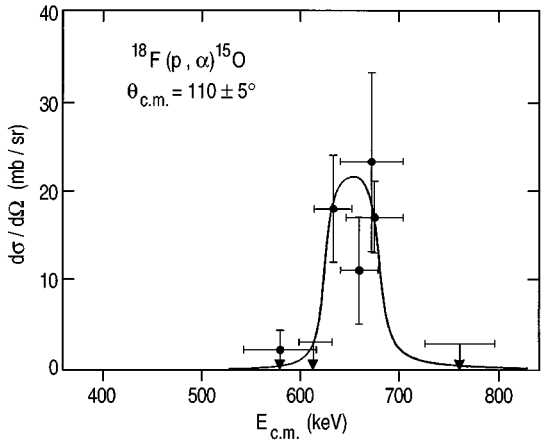

FIG. 2. Cross sections for the $^{18}F(p,\alpha)^{15}O$ reaction measured at various incident energies in the angular range $\theta_{c.m.}=110°\pm5°$. The horizontal error bars represent the respective target thicknesses. The solid line represents the cross section calculated from a resonance with parameters from the second row in Table I averaged over an energy interval of 55 keV (see text for details).

used as targets. The target thicknesses were measured before and after the experiment with a Cf α source. A Si surface barrier detector was used to monitor the hydrogen content of the targets by measuring H- recoils at $\theta_{lab}=30°$. Four ^{18}F samples were studied at bombarding energies of 12.0, 12.4, 12.9, and 13.4 MeV, respectively. Together with the results from our earlier measurements at 11.7, 13.4, and 15.1 MeV [7] cross sections for the $p(^{18}F, ^{15}O)\alpha$ reaction at seven different excitation energies in ^{19}Ne have been obtained covering the energy range from 616 to 795 keV above the threshold for p decay at 6.411 MeV.

Particle identification was obtained using the gas-filled magnet method which gives clean mass and Z identification even for particles with energies of about 500 keV/nucleon. Details for the technique are given in [12]. To improve background suppression the α particles from the $p(^{18}F, ^{15}O)\alpha$ reaction were detected in kinematic coincidence with a 450 mm^2 Si detector, mounted at the appropriate scattering angle. In the experiments of [7] the focal plane counter was a large area parallel-grid gas counter providing position and time-of-flight information. In the present experiment this counter was replaced by an array of 24 5×5 cm^2 position-sensitive Si detectors arranged to cover a 60 cm×10 cm area which measured the position, time of arrival, and the residual energy of the incoming particles [13].

A spectrum of time of flight (TOF) vs magnetic rigidity $B\rho$ is shown in Fig. 1(a), measured at a scattering angle $\theta_{lab}=13°$ and an incident energy of 12.4 MeV. The various particle groups are indicated in the figure. They originate from elastic scattering of ^{18}O and ^{18}F on ^{12}C, from the ^{18}O- and ^{18}F-induced (p,α) reactions producing ^{15}N and ^{15}O, and from ^{12}C and ^{16}O recoil products. Figure 1(b) shows the same spectrum, but with the requirement of a coincidence with the recoil detector mounted at a scattering angle of $\theta_{lab}=60°$. In this coincidence spectrum only ^{15}O and ^{15}N reaction products from the $p(^{18}F, ^{15}O)\alpha$ and the $p(^{18}O, ^{15}N)$

TABLE I. Resonance yields, energies, and total widths obtained from least-squares fits to the measured excitation function.

$\omega\gamma$ (keV)	E_0 (keV)	$E_x(^{19}Ne)$ (MeV)	Γ_t (keV)	Γ_p (keV)	Γ_α (keV)	Remarks
2.7±0.7	653±7	7.064	32±20			This work Three-parameter fit
2.1±0.7	652±4	7.063	13.6±4.6	5±1.6	8.6±2.5	This work $\Gamma_p/\Gamma_\alpha=0.58$
3.7±0.9	655	7.066	40			E_0 and Γ_t fixed [7]
5.6±0.6	638±15	7.049	37±5	13	24	[9]

α reactions and a few random coincidences with ^{18}O particles remain.

III. EXPERIMENTAL RESULTS

The hydrogen content of the polypropylene targets was found to change during the course of the experiment. The cross sections were therefore normalized to the number of elastically scattered hydrogen recoil particles measured in the Si monitor detector. The cross section for elastic scattering of $p+^{18}$O which is typically 90% of the Rutherford value in this energy region was taken from [14]. The absolute angle of the detector was determined from the ratio of the ^{12}C recoil particles and the elastically scattered ^{18}O beam which is a very sensitive measure of the scattering angle. Another method for calculating the (^{18}F, ^{15}O) cross section, which is independent of the hydrogen content in the target, uses the ratio of the ^{15}N and ^{15}O counts [see Fig. 1(a)] together with the measured ^{18}O$(p,\alpha)^{15}$N cross sections [15,16]. The cross sections calculated by these two methods were found to agree within 20%, better than the 30–40 % statistical accuracy.

Figure 2 shows the cross sections measured in this experiment together with the results obtained in [7]. The horizontal bars represent the range of energies due to the energy loss in the target. As shown in [6–9] this resonance has a spin value of $3/2^+$ corresponding to an $l=0$ proton transfer. The solid line represents a Lorentzian averaged over an energy range of 55 keV with parameters obtained from a least-squares fit to the energy-averaged yields as described below. The energy range of 55 keV represents an average value for the different target thicknesses which correspond to energy losses between 40 and 75 keV. Because of this large value for the integration width the least-squares fit with three free parameters (resonance energy, resonance strength, and total width) did not exhibit any sensitivity to the choice of the total width Γ_t. The parameters obtained from this three-parameter fit are given in the top row of Table I.

In order to reduce the number of free parameters we have used the recently measured value for the ratio $\Gamma_p/\Gamma_\alpha=0.58\pm0.06$ [10] in a least-squares fit leaving the resonance energy E_0 and resonance strength $\omega\gamma$ as free parameters. The ratio Γ_p/Γ_α was obtained in [10] from a ^{19}F(^{3}He,t)^{19}Ne* coincidence experiment populating particle-unbound states in ^{19}Ne with the triton detected at $\theta=0°$. Although a $3/2^+$-$7/2^+$ doublet probably exists in ^{19}Ne in this energy region the shape of the angular distribution for the (^{3}He,t) reactions favors the $3/2^+$ state, since as shown in [17,18] (^{3}He,t) angular distributions for $\Delta J=3$ show a minimum at 0°, while $\Delta J=1$ transitions exhibit a maximum. The parameters resulting from this two-parameter fit are given in the second row of Table I.

A contour plot of χ^2 in the E_0-$\omega\gamma$ space is shown in Fig. 3. Varying the Γ_p/Γ_α value between 0.2 and 1.0 did not result in any appreciable changes of the E_0 and $\omega\gamma$ parameters. Values of $\omega\gamma=2.1\pm0.7$ keV, $\Gamma_p=5\pm1.6$ keV, $\Gamma_\alpha=8.6\pm2.5$ keV, and $\Gamma_t=13.6\pm4.6$ keV were obtained for the different particle widths. It should be noted that the value for $\omega\gamma$ is about 45% lower than the previous result of 3.7 ± 0.9 keV obtained in [7]. The reason for this difference is largely that in [7] we had assumed that the total width of the $3/2^+$ resonance was 40 keV. If we analyze the new excitation function with the same constraint of $\Gamma_t=40$ keV, we obtain $\omega\gamma=2.8\pm0.7$ keV consistent, within the uncertainties, with the 3.7 ± 0.9 keV of [7].

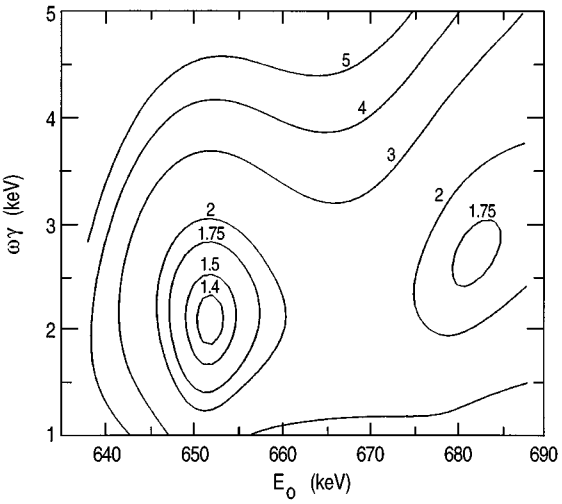

FIG. 3. Two-dimensional plot of the normalized χ^2 in the E_0-$\omega\gamma$ plane as obtained from the analysis of the data shown in Fig. 2.

The results from [9] which were obtained from thick target measurements (see fourth row in Table I) shows values for the resonance strength and the total width which are larger by about a factor of 2. The reason for this discrepancy is not clear. The value for the total width $\Gamma_t=37\pm5$ keV in [9] results in an α width of $\Gamma_\alpha=24$ keV which is considerably larger than the width observed for a $3/2^+$ state at $E_x=7.10$ MeV in the mirror nucleus ^{19}F where from a ^{15}N(α,α) measurement a width of $\sim$8 keV (in the c.m. system) was deduced [19]. This value is in better agreement with the result from our analysis where, with the $\Gamma_p/\Gamma_\alpha=0.58$ constraint $\Gamma_\alpha=8.6\pm2.5$ keV was obtained. The evidence for a $3/2^+$ state at this excitation energy had been questioned in a reanalysis of the data by Mo *et al.* [20]. However, as pointed out in [21] this reanalysis of the ^{15}N(α,α) experiment results in an overprediction of the cross section at most angles. Since both ^{18}F$(p,\alpha)^{15}$O experiments conclude that the data require a $l_p=0,3/2^+$ state in ^{19}Ne around 7.06 MeV the conclusions in [20] have to be questioned.

IV. THE ASTROPHYSICAL REACTION RATE

A $3/2^+$ state in ^{19}Ne formed by $l=0$ protons has a strong influence on the astrophysical reaction rate for the ^{18}F(p,α) reaction. In order to predict this rate the contributions from other states located in the excitation energy region must be considered. Such calculations are complicated by the fact that not all analog states of ^{19}F have been located in the mirror nucleus ^{19}Ne. There are seven states known in ^{19}F between an excitation energy of 6.75 and 7.25 MeV [22]. They are summarized together with their spin values in Table II. The only analog pairs in this region are the $3/2^-$states at 6.742 MeV (^{19}Ne) and 6.787 MeV (^{19}F) and the $7/2^-$ states at 6.861 MeV (^{19}Ne) and 6.927 MeV (^{19}F). For the other cases the excitation energy in ^{19}Ne has been calculated assuming the same Thomas-Ehrman shift as found for the $3/2^-$ pair at 6.787 MeV (^{19}F) and 6.742 MeV (^{19}Ne). A survey of

TABLE II. Energies and widths for various states used in the reaction rate calculations shown in Fig. 4.

J^π	$E_x(^{19}F)$ (MeV)	$E_x(^{19}Ne)$ (MeV)	$E_{c.m.}$ (keV)	Γ_p (keV)	Γ_α (keV)
$3/2^+$	7.10[a]	7.063	652	5.0 ± 1.6	8.6 ± 2.5
$7/2^+$	7.114[b]	7.069[c]	658	3.3×10^{-2} [d]	34[e]
$1/2^-$	6.989[b]	6.944[c]	633	2.3×10^{-2} [d]	53[e]
$7/2^-$	6.927[b]	6.861[b]	450	1.8×10^{-5} [d]	2.5[e]
$3/2^-$	6.891[b]	6.846[c]	435	6.5×10^{-3} [d]	29[e]
$5/2^+$	6.838[b]	6.793[c]	382	8.3×10^{-4} [d]	1.2[e]
$3/2^-$	6.787[b]	6.742[b]	329	9×10^{-4} [d]	2.6[e]

[a][19].
[b][22].
[c]Calculated from the location of the corresponding states in the mirror nucleus ^{19}F.
[d]Assuming $\Gamma_p=0.01\times\Gamma_{\text{single particle}}$ for negative-parity states and $\Gamma_p=0.1\times\Gamma_{\text{single particle}}$ for positive-parity states.
[e]Scaled from the corresponding values of Γ_α in ^{19}F.

the widths for $1/2^-$ and $3/2^-$ states at similar excitation energies in the neighboring nuclei shows that the experimental widths for negative-parity states are typically less than 1% of their single-particle value, while for positive-parity states ($5/2^+$,$7/2^+$) values up to 10% have been observed. This may be explained qualitatively on the basis of the proximity, in this region of excitation energy, of the $2s_{1/2}$ and $1d$ single-particle states, giving rise to a larger value of the strength function, and the distance from the $1p$ and $2p$ single-particle states. Therefore, for lack of any better information on proton widths, we used the rough estimate of $\Gamma_p=0.01*\Gamma_{sp}$ for negative-parity states and $\Gamma_p=0.1*\Gamma_{sp}$ for positive-parity states in the calculations. The alpha widths Γ_α were scaled by penetrabilities from the experimental values of mirror states in ^{19}F, since by isospin symmetry, the reduced widths for α decay of ^{19}Ne states to ^{15}O should be the same as those of ^{19}F decaying to ^{15}N. These data are summarized in Table II.

The reaction rate from an isolated resonance at $E=E_0$ was then calculated from the integral

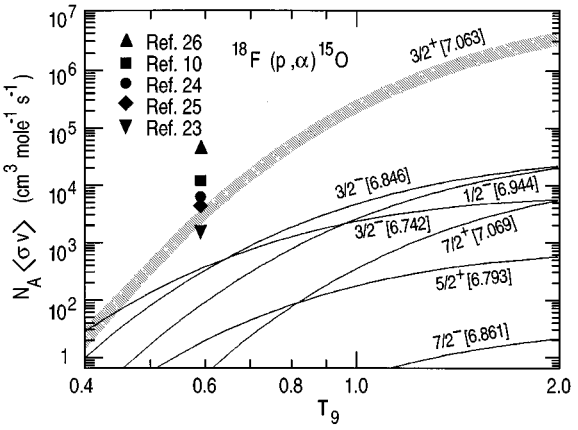

FIG. 4. Astrophysical reaction rate calculated from the resonance parameters for several states with parameters given in Table II. The shaded curve represents the contribution of the $3/2^+$ resonance measured in this experiment. The solid lines are order-of-magnitude estimates for other states, as discussed in the text. The different symbols represent total reaction rates at $T_9=0.6$ from various earlier calculations.

$$N_A\langle\sigma v\rangle=N_A[8/(\pi\mu(kT)^3)]^{1/2}\int_0^\infty\sigma(E)\exp(-E/kT)E\,dE, \tag{1}$$

where

$$\sigma(E)=\pi\lambda\!\!\!^{-2}\omega\,\frac{\Gamma_p(E)\Gamma_\alpha}{(E-E_0)^2+\Gamma_t^2/4}, \tag{2}$$

N_A is Avogadro's number, μ the reduced mass, ω the spin statistical factor associated with the resonance at a c.m. energy E_0, $\Gamma_t=\Gamma_p+\Gamma_\alpha$, and $\lambda\!\!\!^{-}$ the reduced de Broglie wave length, respectively. In the evaluation of the integral the energy dependence of the proton width $\Gamma_p(E)$ has been taken into account. Because of the positive Q value for the (p,α) reaction the α width changes only very little in the energy range of interest and was kept constant. The reaction rate from Eq. (1) is plotted as a function of T_9 in Fig. 4 for each resonance given in Table II.

Since at low temperatures contributions from lower-lying states in ^{19}Ne need to be considered, only the range above $T_9=0.4$ is shown in Fig. 4. One can clearly see that the reaction rate above $T_9=0.5$ is dominated by the $l_p=0,3/2^+$ state at 7.063 MeV. Only at temperatures $T_9<0.5$ do contributions from other states start to be significant with the $3/2^-$ level at 6.742 MeV excitation energy being the most important state.

Earlier estimates [23–26] of the $^{18}F(p,\alpha)^{15}O$ reaction rate at $T_9=0.6$ based on theoretical arguments are shown by the different symbols in Fig. 4. Most of the calculations overpredict the reaction rate by factors up to about 10.

V. SUMMARY

A technique for measurements of nuclear reactions with beams of radioactive species with lifetimes on the order of hours has been developed. It has been used for the case of ^{18}F ($T_{1/2}=110$ min) to measure the low-energy cross section of the $^{18}F(p,\alpha)^{15}O$ reaction which is of interest in explosive nucleosynthesis. Average beam currents of ^{18}F on target on the order of 5×10^5 ions/sec have been produced. A resonance in ^{19}Ne has been found that is likely to dominate the stellar reaction rate for the $^{18}F(p,\alpha)$ reaction in this do-

main. The resonance in ^{19}Ne has $J^{\pi}=3/2^{+}$ at an excitation energy of 7.063 ± 0.004 MeV, and proton and α-particle widths of 5 ± 1.6 and 8.6 ± 2.5 keV, respectively.

The complementary cross section needed for astrophysical models is that for $^{18}\mathrm{F}(p,\gamma)$ reaction. With improvements in the ion source, in the transmission efficiency for the beam, and in particle detection it should be possible to carry out the measurement for $\Gamma_{\gamma}/\Gamma_{p}\sim10^{-3}$. Preparations towards this experiment are under way. Possible ways of extending the technique to other interesting systems are being explored.

This work was supported by the U.S. Department of Energy, Nuclear Physics Division, under Contract No. W-31-109-ENG-38 and the National Science Foundation.

[1] A. E. Champagne and M. Wiescher, Annu. Rev. Nucl. Part. Sci. **42**, 39 (1992).
[2] R. Diel *et al.*, Astrophys. J. Suppl. **92**, 429 (1994).
[3] M. D. Leising and G. H. Share, Astrophys. J. **357**, 638 (1990).
[4] R. K. Wallace and S. E. Woosley, Astrophys. J. Suppl. **45**, 389 (1981).
[5] L. Van Wormer, J. Görres, C. Iliadis, M. Wiescher, and F. K. Thielemann, Astrophys. J. **432**, 326 (1994).
[6] K. E. Rehm *et al.*, Bull. Am. Phys. Soc. **40**, 1033 (1995).
[7] K. E. Rehm *et al.*, Phys. Rev. C **52**, R460 (1995).
[8] R. Coszach *et al.*, in Proceedings of the Meeting of the Belgian Physical Society, Antwerpen, Belgium 1995, Contribution NP6 (unpublished).
[9] R. Coszach *et al.*, Phys. Lett. B **353**, 184 (1995).
[10] S. Utku, Ph.D. thesis, Yale University, 1994, unpublished.
[11] A. Roberts *et al.*, Nucl. Instrum. Methods B **103**, 523 (1995).
[12] K. E. Rehm *et al.*, Nucl. Instrum. Methods A (to be published).
[13] E. R. Jacobsen *et al.*, Nucl. Instrum. Methods A (to be published).
[14] K. Yagi, K. Katori, H. Ohnuma, Y. Hashimoto, and Y. Nogami, J. Phys. Soc. Jpn. **17**, 595 (1962).
[15] H. Lorenz-Wirzba, P. Schmalbrock, H. P. Trautvetter, M. Wiescher, C. Rolfs, and W. S. Rodney, Nucl. Phys. **A313**, 346 (1979).
[16] N. S. Christensen, F. Jensen, F. Besenbacher, and I. Stensgaard, Nucl. Instrum. Methods B **51**, 97 (1990).
[17] J. J. Schwartz and B. A. Watson, Phys. Rev. Lett. **24**, 322 (1970).
[18] A. Richter, J. R. Comfort, N. Anataraman, and J. P. Schiffer, Phys. Rev. C **5**, 821 (1972).
[19] H. Smotrich, K. W. Jones, L. C. McDermott, and R. E. Benenson, Phys. Rev. **122**, 232 (1961).
[20] T. Mo and H. R. Weller, Nucl. Phys. **A198**, 153 (1972).
[21] T. Fortune, J. Phys. G **5**, 381 (1979).
[22] F. Ajzenberg-Selove, Nucl. Phys. **A475**, 1 (1987).
[23] M. Wiescher and K. U. Kettner, Astrophys. J. **263**, 891 (1982).
[24] R. V. Wagoner, Astrophys. J. Suppl. **18**, 247 (1969).
[25] S. E. Woosley, W. A. Fowler, J. A. Holmes, and B. A. Zimmerman, At. Data Nucl. Data Table **22**, 371 (1978).
[26] G. R. Caughlan, unpublished, as quoted in [23].